Microstrip Reflectarray with Elements Having Variable Rotation Angles

John Huang anti Ronald J. Pogorzelski

Jet Propulsion Laboratory
California Institute of Technology
4800 Oak Grove Drive
Pasadena, CA 91109

Key Terms -- reflectarray antenna, microstrip element, variable rotation angle, circular polarization

Abstract -- A novel means of achieving cophasal far-field radiation has been demonstrated for a circularly polarized microstrip reflectarray with elements having variable rotation angles. Two Ka-band, half-meter microstrip reflectarrays have been fabricated and tested. Both are believed to be the electrically largest printed reflectarrays ever developed. One, a conventional design, has identical square patches with variable-length microstrip phase delay lines attached. The other has identical square patches with identical microstrip phase delay lines but different element rotation angles. Both antennas demonstrated excellent performance with more-than-55% aperture efficiencies; but the one with variable rotation angles resulted in better overall performance, A brief mathematical analysis is presented to validate this "rotational element" approach. With this approach, a means of scanning the main beam of the reflectarray over a wide angular region without any RF beamformer by using miniature or micro-machined motors is viable.

1. INTRODUCTION

The most often used conventional high-gain antennas are parabolic reflectors. Although they are efficient radiators, due to their curved reflecting surface, they are generally bulky in size and large in mass. In addition, the main beam of a parabolic reflector can be designed to tilt or scan only a few beamwidths away from its broadside direction, As a remedy, a flat or slightly curved reflector, namely the printed reflectarray, has recently been studied by many researchers. Its reflecting surface can be conformally mounted onto existing supporting structure with relatively small incremental mass and volume. With a proper phase design or phase changing device incorporated into each element of the reflectarray, the main beam can be tilted or scanned to large angles, e.g. 50 degrees, from the aperture broadside direction.

A printed reflectarray antenna consists of two basic elements: an illuminating feed and a thin reflecting surface that can be either flat or slightly curved. On the reflecting surface, there are many printed elements with no power division network, The feed antenna illuminates these elements which are designed to re-radiate the incident field with phases that are required to form a planar phase front. The name "reflectarray" represents an old technology [1], However, the low-profile printed reflectarray is a fairly new concept [2,3,4,5,6], which combines some of the best features of the printed array technology and the traditional parabolic reflector antenna. It provides the low profile and beam scanning [7] capabilities of a printed array and the large aperture with low insertion loss characteristic of a parabolic reflector. There are many forms of printed reflectarray, such as the ones that use identical microstrip patch elements with different-length phase delay lines attached [2,3,7], the ones that use variable-size printed dipoles [5], those use variable-size microstrip patches [6], and those use variable-size circular rings [8,9]. This article presents a new approach for a circularly polarized reflectarray to achieve a far-field beam by using identical microstrip patches having different angular rotations [1 O]. To illustrate the concept, a few elements of the reflectarray are shown in Fig. 1,

It is known that, if a circularly polarized antenna element is rotated from its original position by ψ degrees, the phase of the element will be either advanced or delayed (depending on the rotation direction) by the same ψ degrees, Hence, the technique of rotating circularly polarized elements to achieve the required phases for a conventional array to scan its beam has been previously demonstrated [1 1]. This technique was also demonstrated for a spiraphase reflectarray [12] where discrete and large spiral elements with limited switchable positions were used to scan the beam, Here, small and low-profile printed microstrip elements are used in a reflectarray with continuously-variable angular rotations to achieve far-field phase coherence. When a miniature or micro-machined motor is placed under each microstrip element, this microstrip reflectarray can be controlled to scan its main beam to different and wide angular directions.

Two Ka-band, half-meter diameter, circularly polarized microstrip reflectarrays have been developed. One has identical square patches with variable-length phase delay lines, The other uses identical patch elements with variable element rotation angles. Although both antennas demonstrated excellent efficiencies, adequate bandwidths, and low average sidelobe and cross-pol levels, the one with variable rotation angles achieved superior overall performance. It is believed that these are electrically the largest microstrip reflectarrays (6924 elements with 42 dB of gain) ever developed It is also the first time that circular polarization has been actually demonstrated using microstrip patch elements, Recently, an X-band 0,75 m diameter microstrip reflectarray [13] using variable-length phase delay lines was developed. It demonstrated relatively high efficiency of 70% with peak gain of 35 dB. Although it has dual-linear and dual-circular polarization capabilities, only linear polarization was demonstrated, A 27 GHz microstrip reflectarray using variable-size patches was recently reported [14], It has a diameter of 0,23 m and achieved a gain of 31 dB with an efficiency of 3 10/o. Although dual-linear and dual-circular polarizations can also be achieved by this form of reflectarray, only a linear polarization result was reported. one of the reasons that this 27 GHz reflectarray resulted in a relatively low efficiency is because its efficiency is more susceptible to the fabrication tolerance of the patch dimensions at the high millimeter wave frequency, since the desired phase delays are achieved by varying these patch dimensions, The second reason for its lower efficiency is that phase is achieved at the sacrifice of amplitude. Only one correct dimension will resonate at a particular frequency and, by varying the patch sizes, the amplitudes of many patch elements are sacrificed.

11. ANALYSIS

The analysis carried out here uses conventional array theory without considering mutual coupling and full-wave Scattering; effects. It would not be economical, computation wise, to employ a full-wave technique for thousands of patch elements. Although all the patches are identical with identical phase delay lines, their angular rotations are different, These different rotations do not have repeated pattern in any orthogonal directions ofa rectangular coordinate system; thus the infinite array theory can not be effectively applied here. Fortunately, mutual coupling effect has proven to be negligible in a microstrip array where substrate thickness, dielectric constant, and beam scan angle are not excessively large. Consequently, the analysis here is performed only to determine the required phases for all the elements to achieve a far-field cophasal beam. *No* attempt is made here to accurately calculate the far-field radiation pattern, especially the sidelobe and cross-pol radiations. As will be seen later, the actual sidelobe and cross-pol radiations are strongly affected by the rotation of the elements due to the scatterings of the element structures.

From conventional array theory, when a two-dimensional planar array with M x N patch elements is nonuniformly illuminated by a low-gain feed at r_f, as shown in Fig. 2, the reradiated field from the patches in an arbitrary direction, $\hat{u}$, will be of the form

$$E(\hat{u}) = \sum_{m=1}^{M}\sum_{n=1}^{N} F(\bar{r}_{mn} \cdot \bar{r}_f) A(\bar{r}_{mn} \cdot \hat{u}_o) A(\hat{u} \cdot \hat{u}_o) \exp\left\{ -jk_o\left[\left|\bar{r}_{mn} - \bar{r}_f\right| + \bar{r}_{mn} \cdot \hat{u}\right] + j\alpha_{mn}\right\} \qquad (1)$$

where F is the feed pattern function, A is the pattern function of the patch element, $\bar{r}_{mn}$ is the position vector of the mnth patch, $\hat{u}_o$ is the desired main beam pointing direction, and α_{mn} is the required phase delay of the mnth element, The condition for the aperture distribution to be cophasal in the desired direction $\hat{u}_o$ is

$$\alpha_{mn} - k_o\left[\left|\bar{r}_{mn} - \bar{r}_f\right| + \bar{r}_{mn} \cdot \hat{u}_o\right] = 2n\pi, \qquad n = 0, 1, 2, \cdots \qquad (2)$$

For a circular aperture as shown in Fig. 2, which is more desirable for better aperture efficiency (less spillover 10SS) than a rectangular aperture, the summation signs in Eq. (1) can be truncated (no calculation) for patches located outside the circular aperture. Eq.(2) gives the phase delays of all the elements for a reflectarray to achieve a far-field co-phasal beam. The following analysis presents the amount of angular rotation needed by a circularly polarized (C.P.) element to achieve the phase delay required by Eq. (2).

Consider the case as shown in Fig. 3(a) where the two transmission phase delay lines connected to the square patch are of unequal lengths, l_x and l_y, but where the lengths are uniform across the reflectarray aperture. For now, let's consider that the two lines are short-circuit terminated and let the reflectarray be illuminated by a left C.P. and normally incident plane wave propagating in the negative z direction. This incident wave may be expressed as

$$\bar{E}^{inc} = (\hat{u}_x + j\hat{u}_y)\, a\, e^{-jkz} e^{-j\omega t} \tag{3}$$

The reflected wave may be written in the form,

$$\bar{E}^{refl} = (-\hat{u}_x e^{2jkl_x} - j\hat{u}_y e^{2jkl_y})\, a\, e^{jkz} e^{-j\omega t} \tag{4}$$

where the minus signs arise from the reflection coefficients of -1 at the short-circuit terminations, "a" is the amplitude and attenuation is assumed to be zero in the patch and the lines. Note that, when $l_x = l_y$, the incident left C.P. plane wave is converted upon reflection into a right C.P. plane wave in the usual manner by virtue of the reversal of the direction of propagation. Now, let one delay line be longer than the other by 90-deg; for example, $kl_x = \pi/2$ and $kl_y = 0$. Then the reflected wave will be

$$\bar{E}^{refl} = (\hat{u}_x - j\hat{u}_y)\, a\, e^{jkz} e^{-j\omega t} \tag{5}$$

which is a left C.P. wave just as was the incident wave

Now let the element be rotated by angle ψ, shown in Fig. 3(b), so as to align with the axes of a new coordinate system (x', y'). The excitation of each of the two orthogonal component fields in each patch can be deter-mined by projecting the $\hat{u}_x$ and $\hat{u}_y$ field components onto the $\hat{u}_{x'}$ and $\hat{u}_{y'}$ axes at $z = 0$. That is

$$\begin{aligned} \bar{E}^{inc}\Big|_{z=0} &= \Big[\left(\hat{u}_{x'}\cos\psi - \hat{u}_{y'}\sin\psi\right) + j\left(\hat{u}_{x'}\sin\psi + \hat{u}_{y'}\cos\psi\right)\Big]\, a\, e^{-j\omega t} \\ &= \left(\hat{u}_{x'} e^{j\psi} + j\hat{u}_{y'} e^{j\psi}\right) a\, e^{-j\omega t} \end{aligned} \tag{6}$$

The reflected wave now becomes

$$\bar{E}^{refl} = -\left(\hat{u}_{x'} e^{2jkl_{x'}} + j\hat{u}_{y'} e^{2jkl_{y'}}\right) a\, e^{jkz} e^{j\psi} e^{-j\omega t} \tag{7}$$

where, again, the minus sign arises from the reflections at the transmission line short circuit terminations. Finally, re-expressing the reflected field in terms of the original x and y components yields,

$$\bar{E}^{refl} = -\left[\left(\hat{u}_x \cos\psi + \hat{u}_y \sin\psi\right)e^{2jkl_{x'}} + j\left(-\hat{u}_x \sin\psi + \hat{u}_y \cos\psi\right)e^{2jkl_{y'}}\right] a\, e^{jkz} e^{-j\omega t} e^{j\psi} \qquad (8)$$

which, via some algebraic manipulation, can be written in the form,

$$\bar{E}^{refl} = -\frac{1}{2}\left[\left(e^{2jkl_{x'}} - e^{2jkl_{y'}}\right)\left(\hat{u}_x - j\hat{u}_y\right)e^{2j\psi} + \left(e^{2jkl_{x'}} + e^{2jkl_{y'}}\right)\left(\hat{u}_x + j\hat{u}_y\right)\right] a\, e^{jkz} e^{-j\omega t} \qquad (9)$$

Note that this reflected wave has both left and right circularly polarized components and that the right circularly polarized component is independent of the rotation angle of the elements. If we now select transmission line lengths differing by a quarter wavelength; for example, $kl_{x'} = \pi/2$ and $kl_{y'} = 0$, then the right circularly polarized component of the reflected wave is eliminated and the remaining left circularly polarized component becomes,

$$\bar{E}^{refl} = \left(\hat{u}_x - j\hat{u}_y\right) a\, e^{jkz} e^{-j\omega t} e^{2j\psi} \qquad (10)$$

l'bus, the reflected wave has been delayed in phase (path lengthened) by 2 ψ radians due to element rotation by angle ψ. By carry out the same derivation, one will note that a right C.P. incident wave would be phase advanced upon reflection, If the transmission lines had been terminated in open circuits instead of short circuits, the reflected wave would be opposite in sign, but not opposite in sense, from that of Eq. 10, To summarize, Eq. *10* implies that the needed phase delay of *2* ψ degrees from a C.P. patch element shown in Fig. 3 would require a counter-clockwise angular rotation of ψ degrees by the element.

III. ANTENNA DESIGN AND DEVELOPMENT

Two Ka-band, circularly polarized microstrip reflectarrays have been designed, fabricated, and tested at JPL. Each one has a diameter of a half meter and 6,924 square patch elements. One, designed with the conventional approach, has identical patches but with variable-length phase delay lines, The other one, shown in a photograph in Fig. 4, also uses identical patches but with variable patch rotation angles. Both antennas have patch elements etched on Duroid substrates with 0.254 *mm* thickness and *2,2* relative dielectric constant. With this substrate thickness and dielectric constant, the predicted patch bandwidth is about 4 percent. Both antennas were designed for broadside radiation with the same f/D ratio of *0.75*, *"f"*, being 37.2 cm long, is the focal length and is the distance between the phase center of the feed horn and the radiating plane of the patch elements. "D" is the diameter of the radiating aperture and is equal to 50 cm. Each patch element has a square dimension of 2.946 mm and was designed and tested to resonate at 32.0 GHz. The element spacing is 0.58 free-space-wavelength which was determined to avoid grating lobes. This element spacing was also determined to allow appropriate real estate for the rotation of the elements so that no two neighboring elements will physically interfere each other. The widths of all the microstrip phase delay lines are identical and is 0.075 mm which was designed to have an impedance of 150 ohms. The input impedance of the square patch was measured to be 230 ohms. Although it is not critical, the line impedance should be as close to the input impedance of the patch as possible so that mismatch and multiple reflections within the line are minimized. To have a line impedance equal to 230 ohms would yield an extremely thin line width at the Ka-band frequency, which would present serious reliability and fabrication issues, Too thin a line could be easily scratched or delaminated. In addition, due to etching tolerance, it would be more difficult to maintain uniformity of line width across the large aperture if the lines were too thin. Consequently, a compromising 150-ohm line was selected. The etching tolerance achieved across the entire aperture for both patch and phase delay line is ±0.008 mm. A great deal of effort was spent in assuring the achievement of this tolerance,

To assure good antenna efficiency and no surprisingly high sidelobes, the radiating aperture of the reflectarray should maintain a flatness of at least l/30th of a wavelength, which is 0,3 mm. In order to achieve this flatness across the half-meter aperture, the thin Duroid substrate is supported by a 1.9-cm thick aluminum honeycomb panel. To each side of the panel is bonded a 0,5-mm thick graphite epoxy face sheet. The etched copper-clad Duroid substrate is then bonded onto one face sheet. The feed horn, which is a circularly polarized corrugated conical horn, is precision fastened above the honeycomb panel by four 1 -cm-diameter aluminum rods, This feed horn was designed to illuminate the reflectarray aperture with a -9 dB edge taper. The -3 dB and -9 dB beamwidths of the feed horn are 41 -deg and 69-deg, respectively. The purpose of the feed horn's corrugation is to reduce sidelobes for lower spillover loss and to minimize cross-pol levels for better polarization efficiency. This well designed feed horn is one of the primary reasons that the reflectarray achieved good overall antenna efficiency.

IV, MEASUREMENT RESULTS

For the sake of convenience, from here on, the reflectarray with patches having variable-length phase delay lines is named "unit 1", and the one with patches having variable rotation angles is named "unit 2". The radiation pattern of unit 1, measured at 32,0 GHz, is given in Fig. 5, which shows a peak sidelobe level of -22 dB and all other sidelobes, except the first two, are well below -30 dB level. This indicates that the undesirable backscattered fields (from patches, phase delay lines, ground plane edges, etc.) are insignificant compared to the desirable reradiated field. This, in turn, indicates that the patches are well matched in impedance to the phase delay lines and the fabrication accuracy is well controlled. The two high sidelobes adjacent to the main beam are believed to be caused by the feed structure blockage, All the cross-pol radiations in Fig. 5, except within the main beam region, are well below -40 dB level. The relatively high cross-pol of -22 dB in the main beam region is caused by the co-phasal behavior of the cross-pol components of the patches anti the cross-pol of the feed horn In other words, the cross-pol fields, similar to the co-pol fields, are all coherently directed to the same direction by the same set of phase delay lines, This phenomenon can be verified by the results of unit 2 whose measured pattern is presented in Fig. 6, This unit 2 also shows a peak sidelobe of -22 dB which is expected due to the same feed structure blockage. All the other sidelobes, except the first few, are well below -40 dB and are significantly lower than those of unit 1. The cross-pol radiation of unit 2, except one cross-pol lobe at -28 dB, are all below -30 dB. It seems that the single high cross-pol lobe in the main beam of unit 1 has now disappeared in unit 2 and is distributed over a wide angular region at lower levels outside the main beam region, One major reason that unit 2 achieves lower sidelobe and cross-pol levels than those of unit 1 is the diffuse, instead of the cophasal, scattering by the near randomly rotated patches. Although the rotations of all patches have electrically a unique pattern for the co-pol field, they appear physically to be randomly rotated to the structurally scattered fields and the cross-pol field,

At 32.0 GHz, the measured -3 dB beamwidth of unit 1 is 1. 18-deg and the measured gain is 41.75 dB which corresponds to an overall antenna efficiency of 53 percent. For this unit, the patterns and antenna gains were measured over the frequency range between 31.0 GHz and 33.0 GHz. Across this frequency range, all the patterns, except toward the high end where significant pattern degradation starts to occur, exhibit features similar to those shown in Fig. 5. At 31.5 Ghz, unit 1 achieved its highest gain of 42.75 dB which translates to an efficiency of 69 percent. 'l'he measured antenna gain and efficiency versus frequency curves for unit 1 are presented in Fig. 7 where an oscillatory response is observed for each curve. It is believed that, in addition to the resonance of the patches, some of the phase delay lines also become resonant at a particular frequency since they have length dimensions close to those of the patches, This is illustrated in a close-up view of the reflectarray elements in Fig. 8, The resonances of these lines add in-and-out of phase with the resonance of the patches over the above frequency range and may thus cause the oscillatory behavior. One way to avoid this oscillatory behavior is to place the phase delay lines behind the ground plane in an additional substrate layer. Another way, to be detailed later, is to use the rotational technique adopted in unit 2, Figure 7 exhibits a ± 1 dB gain (around a nominal gain of 41,75 dB) bandwidth of 1,0 GHz which is about 3 percent and a -3 dB gain (from the peak gain of 42.75 dB) bandwidth of 1,8 GHz which is about 5.6 percent.

Unit 2 has a -3 dB beamwidth of 1.2-deg at the designed center frequency of 32.0 GHz where the measured gain is 41,7 dB for an efficiency of 52 percent. "l'his unit, similar to unit 1, seems to operate better at slightly lower than the design frequency. Over the frequency range of 31.0 GHz to 33,0 GHz, unit 2 shows a peak gain of 42,2 dB at 31,7 GHz. "l'his gain cot-responds to an antenna efficiency of 60 percent which, as a large array of several thousand elements at the Ka-band frequency, is considered quite good. 'l'he bandwidth behavior of this unit is presented in Fig. 9 where a -1 dB gain bandwidth of 1,1 GHz (3.5 percent) and a -3 dB gain bandwidth of 1.7 GHz (5.4 percent) are demonstrated, Except for the oscillatory behavior of unit 1, the bandwidths of both units are very similar and are quite adequate for most telecommunication applications at Ka-band. Wider bandwidth [1 O] can be achieved by re-designing the patch elements, using larger f/D ratio, or employing time delay, instead of phase delay, lines. One major difference between the curves of Fig. 7 and Fig. 9 is that the oscillatory behavior of the curves for unit 1 has diminished in the curves for unit 2. "l'his is because not only do all the patches of unit 2 have identical phase delay lines but also they appear to be randomly rotated. As a result, it is not likely that the phase delay lines of unit 2 could resonate with the patches in-and-out of phase many times across a frequency band. To summarize, the unit 2 antenna has achieved overall better performance than that of unit 1, By using rotational elements, the unit 2 microstrip reflectarray has demonstrated lower sidelobes, lower cross-pol radiation, and better bandwidth behavior.

V. CONCI.USION

A Ka-band, high gain, circularly polarized microstrip reflectarray antenna has demonstrated superior performance with variably rotated elements, Its sidelobes are mostly below the -40 dB level and most of its cross-pol radiation is below the -30 dB level. A peak efficiency of 60 percent has been achieved. By utilizing the rotational technique presented here, a novel beam scanning method is proposed. By incorporating a miniature or micro-machined motor underneath each element and, thereby, actively rotating all the elements, a circularly polarized microstrip reflect array can have its main beam scanned to wide angles, With this scanning method, no insertion loss will be added to the system, such as that of the phase shifter loss in a conventional phased array. Consequently, the expensive T/R modules that are generally needed in a conventional phased array system are not required here. '1'bus, a relatively lower cost and more efficient beam scanning array antenna maybe realized,

References:

1. D. G. Berry, R. G, Malech, and W, A, Kennedy, "'l'he Reflectarray Antenna," IEEE Trans. Antennas and Propagat., Vol. AP- 11, pp. 645-651, November 1963.

2. R. E. Munson and H. Haddad, "Microstrip Reflectarray for Satellite Communication and RCS Enhancement and Reduction, " U.S. Patent 4,684,952, Washington D.C., August 19s7.

3. J. Huang, "Microstrip Reflectarray Antenna for the SCANSCAT Radar Application," JPL publication 90-45, November 1990.

4. J. Huang, "Microstrip Reflectarray," IEEE AP-S Symposium, London, Ontario, Canada, pp. 612-615, June 1991,

5. A. Kelkar, "FLAPS: Conformal Phased Reflecting Surfaces," Proceedings of the IEEE National Radar Conference, pp. 58-62, March 1991,

6. D. M. Pozar and T. A. Metzler, "Analysis of a Reflectarray Antenna Using Microstrip Patches of' Variable Size," Electronics Letters, pp. 657-658, April 1993.

7, R. D. Javor, X. D. Wu, and K. Chang, "Beam Steering ofa Microstrip Flat Reflectarray Antenna," IEEE AP-S Symposium, pp. 956-959, June 1994.

8. F. S. Johansson, "Frequency-Scanned Reflection Gratings Consisting of Ring Patches," IEE Proceedings, Vol. 138, No. 4, pp. 273-276, August 1991.

9. Y. J. Guo and S. K. Barton, "Phase Correcting Zonal Reflector Incorporating Rings,>' IEEE Trans. Antennas and Propagat., Vol. 43, pp. 350-255, April 1995.

10. J. Huang, "Bandwidth Study of Microstrip Reflectarray and a Novel Phased Reflectarray Concept," IEEE AP-S Symposium, Newport Beach, CA, pp. 582-585, June 1995,

11. M. 1.. Oberhart and Y. '1', Lo, "Simple Method of Experimentally Investigating Scanning microstrip Antenna Arrays Without Phase-Shifting Devices," Electronics Letters, pp. 1042-1043, August 19S9,

12. H. R. Phelan, "Spiraphase Reflectarray-for Multitarget Radar," Microwave Journal, pp. 67-73, July 1977,

13. D. C. Chang and M. C. Huang, "Multiple Polarization Microstrip Reflectarray Antenna With High Efficiency and Low Cross-Polarization," IEEE Trans. Antennas and Propagat., Vol. 43, pp. 829-834, August 1995.

14. S, D. Targonski and D. M. Pozar, "Analysis and Design of Millimeter Wave Microstrip Reflectarrays," IEEE AP-S Int. Symp. Digest, pp. 578-581, June 1995,

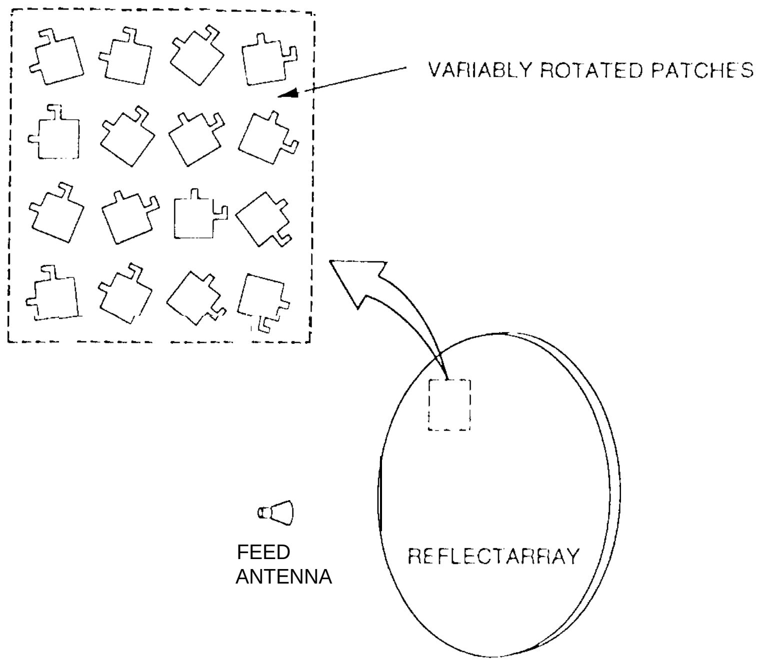

Figure 1, Circularly polarized microstrip reflectarray with elements having variable rotation angles.

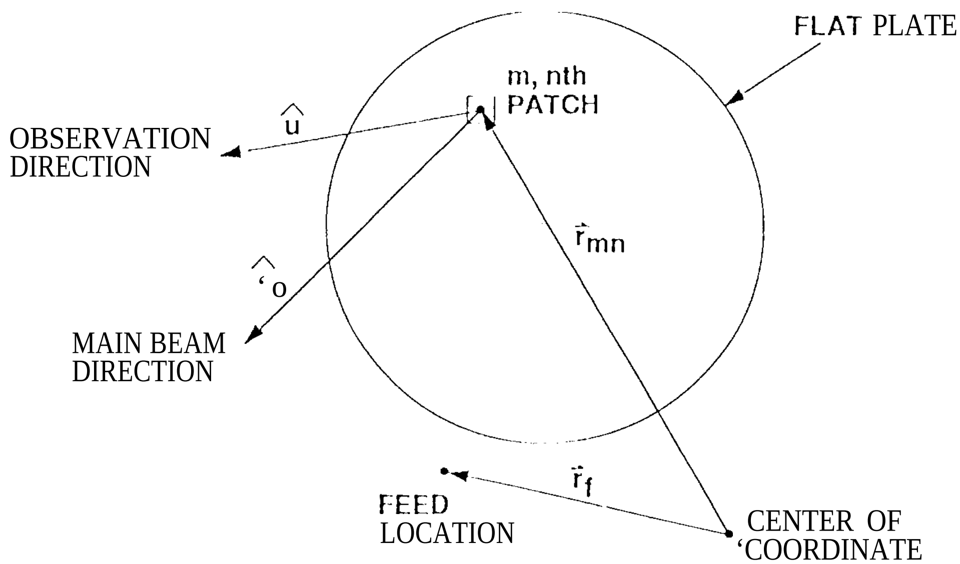

Figure 2. Coordinate system for reflectarray pattern analysis,

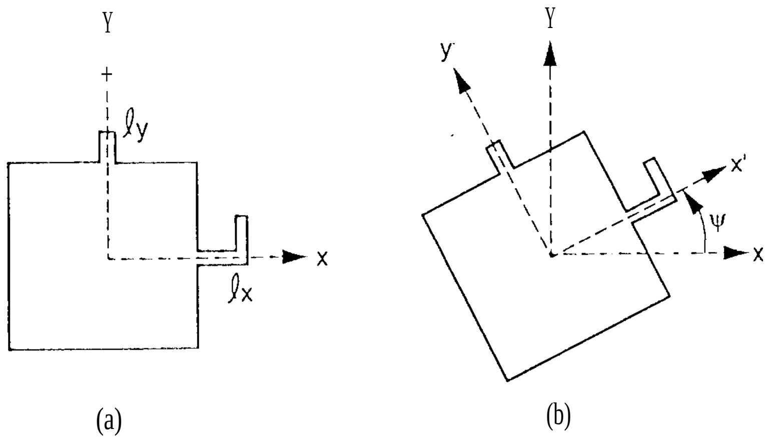

Figure 3 Circularly polarized reflectarray patch element; (a) reference element with 0° phase shift, (b) ψ-deg rotated element with 2 ψ-deg phase shift.

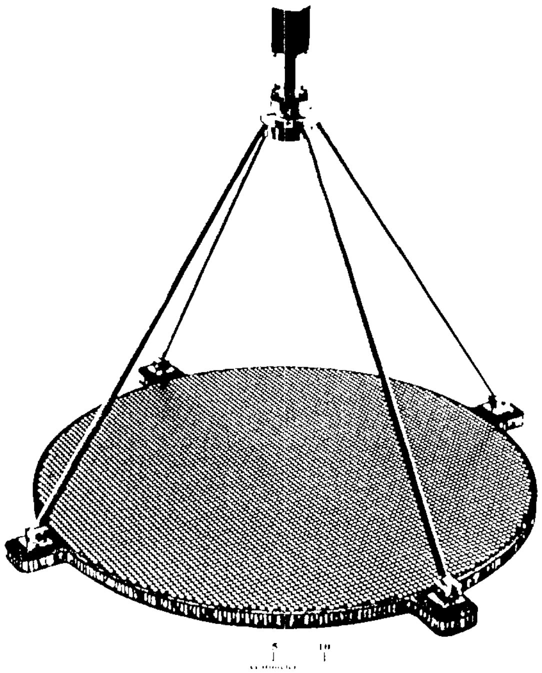

Figure 4. Photograph of the half meter Ka-band microstrip reflectarry with elements having variable rotation angles.

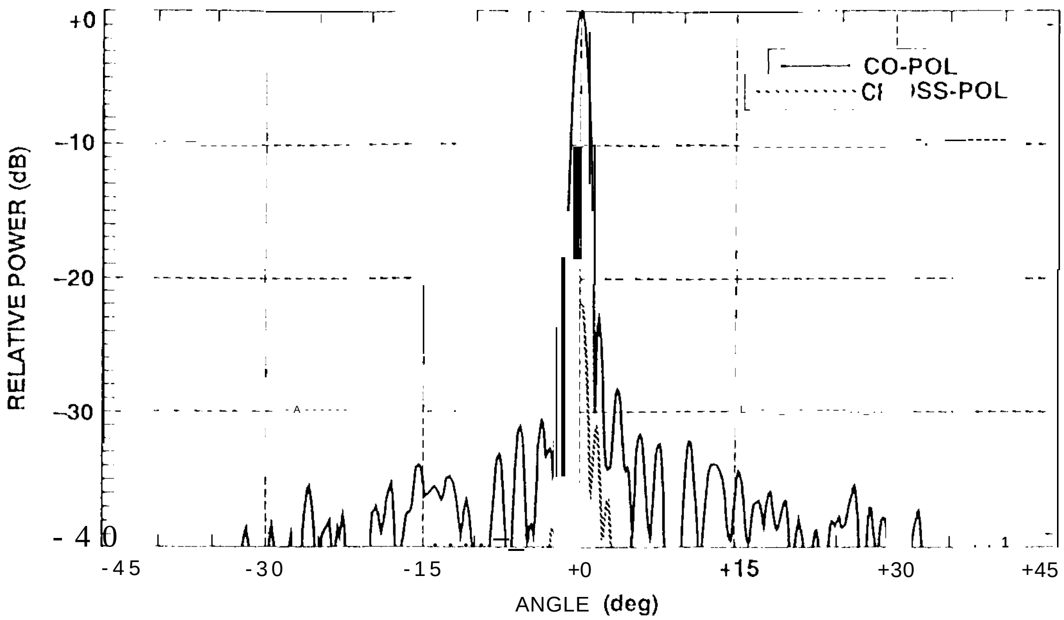

Figure 5. Measured radiation pattern of unit 1 reflectarray with patches having variable-length phase delay lines; frequency = 32.0 GHz.

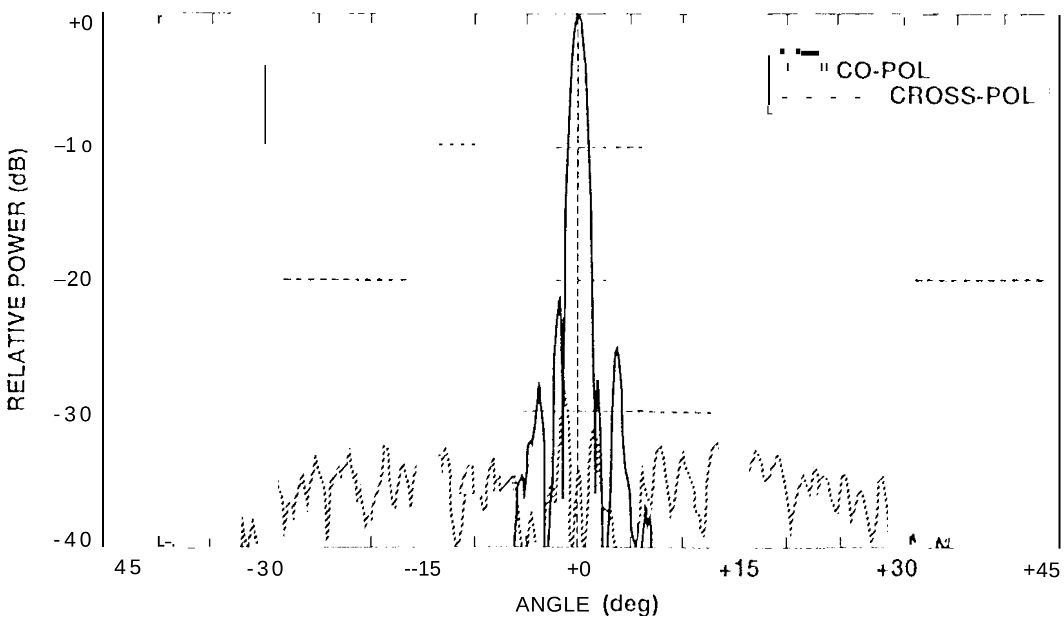

Figure 6. Measured radiation pattern of unit 2 reflectarray with patches having variable rotation angles; frequency = 32.0 GHz.

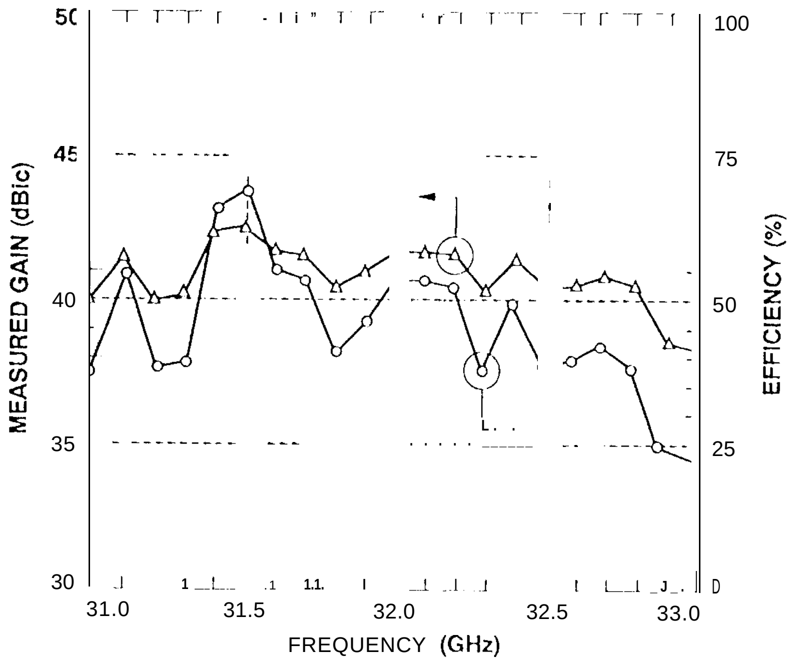

Figure 7. Measured bandwidth characteristics of unit 1 reflectarray with patches having variable-length phase delay lines,

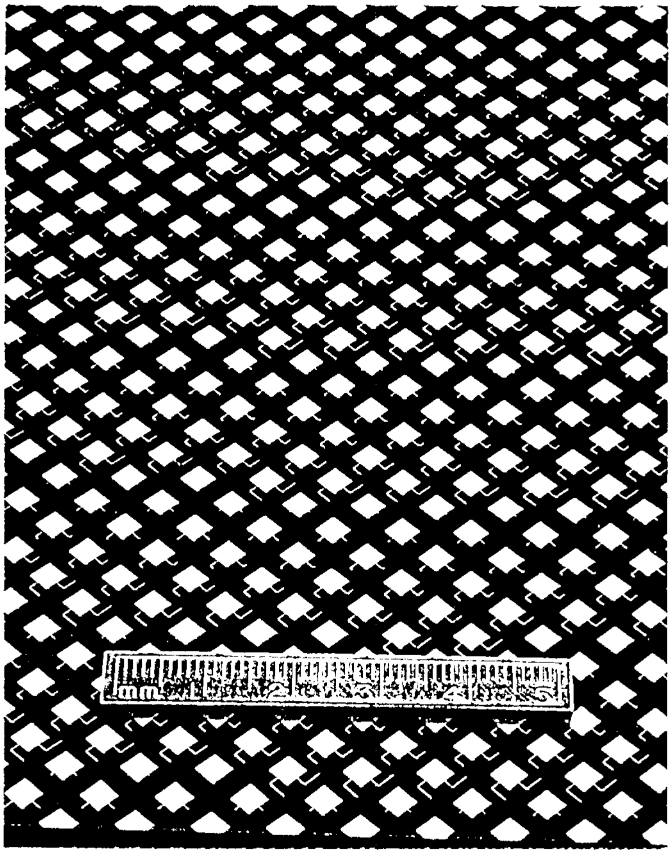

Figure 8. Close-up view of unit 1 reflectarray showing some elements with phase delay lines having similar linear dimensions as the patch,

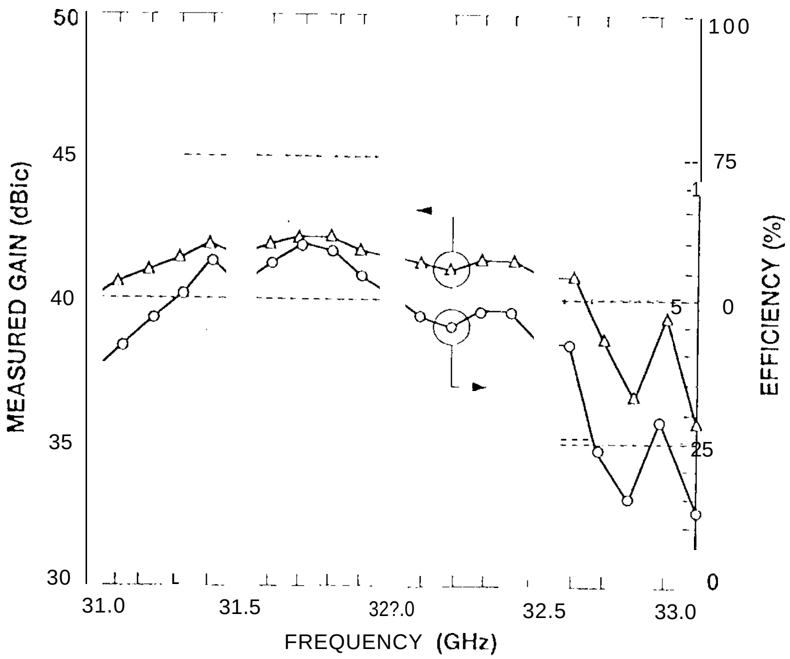

Figure 9. Measured bandwidth characteristics of unit 2 reflectarray with patches having variable rotation angles.